International Journal of GEOMATE, Dec., 2019 Vol.17, Issue 64, pp. 63 - 70
ISSN: 2186-2982 (P), 2186-2990 (O), Japan, DOI: https://doi.org/10.21660/2019.64.78237
Geotechnique, Construction Materials and Environment

ASSESSMENT OF ELEVATED TEMPERATURE EFFECTS ON SELF-COMPACTING AND HIGH-STRENGTH CONCRETE BEAMS IN COMPARISON WITH NORMAL CONCRETE BEAMS

*Ahmed Hassan[1], Laila Abd-EL-Hafez[2, 3], Alaa Abouelezz[2] and Faisal Aldhafairi[2]
[1]Civil Engineering Department, Beni-suef University, Egypt.
[2]Civil Engineering Department, Minia University, Minia, Egypt.
[3]Civil Engineering Department, Nahda University, Beni-suef, Egypt.
*Corresponding author, Received: 28 May 2019, Revised: 10 July 2019, Accepted: 15 Aug. 2019

ABSTRACT: Developments in the concrete industry have allowed for the use of concrete types other than conventional concrete, such as self-compacting and high-strength concrete. Conventional concrete beams exhibit a significant reduction in strength following fire exposure. This study includes experimental and theoretical components. An experimental program was designed to investigate the effects of different elevated temperature levels on the most common concrete types. A total of 15 beams were cast using normal, self-compacting, and high-strength concrete beams. Moreover, 12 beams were subjected to temperatures of 400 °C and 600 °C for 1 and 2 h to study the beam behavior under indirect fire conditions. The exposure time had a significant effect on the behaviour of the different beams, particularly the normal concrete, which exhibited a dramatic strength reduction after being subjected to a temperature of 600 °C for 2 h. The self-compacting concrete beam demonstrated acceptable behavior under elevated temperature conditions up to 600 °C. Strong agreements were observed between the experimental results and theoretical analysis, which was performed by the finite element program ANSYS.

Keywords: Elevated temperature, Normal concrete, Self-compacting concrete, High-strength concrete.

1. INTRODUCTION

In recent years, developments in the concrete industry have led to self-compacting concrete (SCC) and high-strength concrete (HSC) being the main types of concrete in use in addition to normal concrete (NC). Numerous studies have been conducted to investigate the effects of elevated temperatures on the concrete elements. The strength reduction of HSC following elevated temperature exposure leads to losses in smaller specimens [1]. The residual mechanical properties of self-compacting and high-strength concrete are similar to those of conventional HSC [2], while the risk of spalling in self-compacting high-strength concrete is greater than that of conventional HSC. By increasing the temperature level, the hot compressive strength of SCC is decreased [3]. The concrete grade has a significant effect on its residual strength, especially at temperatures less than 400 °C. A greater strength reduction has been reported with higher SCC grades. However, this difference was found to be smaller in the permanent strength loss stage [3]. The temperature distribution through the cross-sections was evaluated by a simplified approach for reinforced concrete members under fire exposure [4]. The cooling method has a direct effect on the flexural strength and residual compressive strength, with the effect being more pronounced as the temperature increases [5]. Moreover, the weight of the specimens is significantly reduced with an increase in temperature, and this reduction is very sharp beyond 800 °C. The effects of the water/cement ratio and aggregate type on the weight losses have not been found to be significant. Results have also revealed that the relative strength of concrete decreases as the exposure temperature increases [6]. Traditional concrete exposed to high temperature undergoes a series of physicochemical changes in its structure, causing a gradual to a sharp loss in its mechanical strength and durability, cracking, and sometimes spalling [5–7]. Data compiled from fire experiments indicated clear performance differences between SCC and traditional concrete at elevated temperatures, owing to differences in the microstructural properties, represented in the porosity, pore size distribution, and pore connectivity [8, 9]. Most recently published works have been directed towards understanding the thermal performance of SCC, with an emphasis on the microstructure, phase composition, and mechanical and thermal properties [10–12].

In this study, to evaluate the performance of the different concrete types, namely NC, SCC, and HSC, 15 beams were cast and tested. The temperature levels applied were 400 °C and 600 °C, for 60 and 120 min exposure times.

2. EXPERIMENTAL PROGRAM

2.1 Geometric And Material Configurations Of Test Specimens, And Investigated Parameters

Rectangular cross-sections of reinforced concrete beams were cast with a size of 120 mm (width) × 300 mm (height) × 1400 mm (length). All beams had the same reinforcement: two bars of 10 mm in diameter was used for the bottom and top reinforcement, and 8 mm diameter stirrups were used for the shear resistance, spaced at 8 cm, as illustrated in Fig. 1. Two different elevated temperature levels of 400 °C and 600 °C were applied for 1 and 2 h to study the effects of the elevated temperature levels and durations. An electrical furnace was used to expose the specimens to the suggested temperature level rates. The furnace temperature rates were compatible with ASTM 119 [13], as indicated in Fig. 2. Following exposure to elevated temperatures, the reinforced concrete beams were allowed to cool gradually for 1 d. Three-point flexural tests were used to evaluate the reduction in the beam capacity following elevated temperature exposure in the control beams. The remaining beams were retrofitted by the steel jacket and CFRP laminate techniques and then tested to assess the behavior and beam capacity restoration in comparison with the unheated control beams. Table 1 presents all of the specimens, conditions, and coding.

Fig.1 Geometry and steel reinforcement for tested beam

Table 1 Specimen coding for concrete beams

Specimen	Temperature	Duration
N	25°	-------
N 400 1 h	400°	1 h
N 400 2 h	400°	2 h
N 600 1 h	600°	1 h
N 600 2 h	600°	2 h
S	25°	-------
S 400 1 h	400°	1 h
S 400 2 h	400°	2 h
S 600 1 h	600°	1 h
S 600 2 h	600°	2 h
H	25°	-------
H 400 1 h	400°	1 h
H 400 2 h	400°	2 h
H 600 1 h	600°	1 h
H 600 2 h	600°	2 h

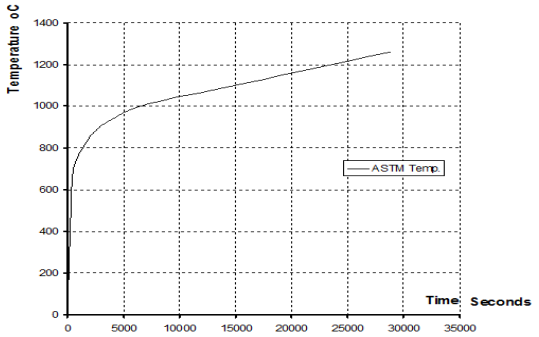

Fig.2 ASTM 119 fire exposure testing curve [13]

2.2 Material Properties And Concrete Mix Preparations

The compressive strength of the HSC beams was designed to achieve 60 MPa, while the NC and SCC mixes were designed to have the same grade of 30 MPa. The main materials used for casting all concrete beams consisted of Portland cement, equivalent to ASTM Type I, natural water, and natural aggregates. The NC contained gravel as the coarse aggregate, as reported in Table 2, while the SCC and HSC were made using dolomite, as indicated in Tables 3 and 4. A concrete rotating drum mixer with a full capacity of 0.125 m3 was used to mix the concrete contents. For the different concrete types, the coarse aggregate, sand, and cement were dry mixed for 2 min. Following the dry mixing, water was gradually added to ensure that the concrete became homogeneous. For the SCC, silica fume was used to increase the density, compressive strength, and durability of the concrete, as well as to improve the fresh concrete performance with increased workability, and improved cohesiveness and stability. Sika ViscoCrete® -3425 is a third-generation super plasticizer for homogenous concrete, and is considered as a powerful super plasticizer that acts by means of different mechanisms. Sika Fiber is a monofilament polypropylene fiber for use in concrete mixes, which reduces the tendency of plastic and drying shrinkage cracking, improves the abrasion resistance, reduces water migration, improves durability, reduces spalling, and increases the impact resistance of young concrete. The dolomite, sand, silica fume, and cement were dry mixed. Thereafter, water was gradually added to the Sika ViscoCete -3425 and Sika Fiber, while mixing was performed for an additional 2 min, following which the concrete became homogeneous. Cubes of 150 mm and cylinders with dimensions of 150 × 300 mm were cast to investigate the concrete mechanical properties at room temperature and after exposure to elevated temperatures of 400 °C

and 600 °C. The ACI specifications were followed in the casting and curing system [14].

Table 2 NC mix proportions

fc (MPa)	w/c ratio	Cement (kg/m3)	Coarse aggregate (kg/m3)	Fine aggregate (kg/m3)	Addicrete Bvf (LT/m3)
30	0.43	400	1160	578	8%

Table 3 SCC mix proportions

fc (MPa)	w/c ratio	Cement (kg/m3)	Coarse aggregate (kg/m3)	Fine aggregate (kg/m3)	Silica fume (kg/m³)	Sika ViscoCrete (kg/m³)	Sika Fiber (G) (kg/m3)
30	0.36	310	650	650	35	4	0.90

Table 4 HSC mix proportions

fc (MPa)	w/c ratio	Cement (kg/m3)	Coarse aggregate (kg/m3)	Fine aggregate (kg/m3)	Silica fume (kg/m³)	Superlitter Addicrete Bvf
60	0.35	525	1200	550	78	4%

2.3 Experimental Program Setup And Testing

A 1000 kN universal testing machine was used to perform three-point flexural tests on the beams, while elevated temperature tests were conducted using a 1200 °C electrical furnace, as illustrated in Fig. 3. The central deflections of the tested beams were recorded using a linear variable differential transformer at the beam centre. The strains were monitored using two strain gauges at different locations: critical flexural strain was expected at the beam centre and maximum shear at a distance equal to the beam depth from the beam support, as illustrated in Fig. 3.

Fig. 3 Furnace and loading test setup

3. RESULTS AND DISCUSSION

The results of the tested beams are reported to assess the effects of elevated temperatures on the different concrete beam types.

3.1. Compressive And Split Tensile Strengths

Table 5 presents the mechanical properties of the different concrete types according to the design mix prepared prior to testing. The SCC and NC had approximately the same properties for reporting the difference after fire exposure.

Table 5 Compressive and tensile strengths of different concrete types

Concrete type	Compressive strength (MPa)		28-day tensile strength (MPa)
	7 days	28 days	
NC	26	31.2	3.1
SCC	27	31.6	3.15
HSC	50	62	5.8

3.2. External Evaluation Following Elevated Temperature Exposure For Different Types Of Reinforced Concrete Beams

An exposure time of 1 h did not result in noticeable changes for all beams exposed to 400 °C for all tested concrete types while increasing the elevated temperature level to 600 °C for 1 h had a significant effect on the NC. Concrete spalling started at 1 h for the NC, and hair cracks were observed for the SCC and HSC, as illustrated in Fig. 4. The color of the beam surface tended to be grey after exposure to 400 °C for 2 h, while the colour of the beams exposed to 600 °C for 2 h tended to be white grey. The spalling and cracks

increased when increasing the exposure time for the NC, SCC, and HSC, as indicated in Fig. 5. These changes could be associated with the change in the concrete composition and texture, which were destroyed during heating, or the oxidization process, which occurred in the ferric components [15, 16]. At the start of cooling after the elevated temperature time, horizontal cracks in the external concrete surface with a full beam width were observed nearly at the location of each stirrup, as illustrated in Fig. 5. This is attributed to the thermal stresses induced in the beams by the difference between the thermal expansion coefficient of concrete and steel reinforcement. The increase in the elevated temperature exposure type to 2 h at 600 °C affected the HSC and SCC, with two or three transferee cracks appearing at the beam surface. These crack started at 400 °C for the SCC beams with a 2 h exposure time. The NC beams exhibited a noticeable deterioration at 400 °C after a 2 h exposure time, and significant and dramatic aggregate spalling at 600 °C after 1 and 2 h, respectively. Aggregate spalling of the NC beams occurred slightly at 400 °C and very significantly at 600 °C. Violent and non-violent breaking off of concrete pieces from the structural element surface occurred at 600 °C and 400 °C, respectively, and these results agree with those of previous studies [17].

At elevated temperatures, the exposed concrete surfaces were significantly affected. Internal stresses and thus cracks of varying sizes were generated owing to the inhomogeneous volume dilatations of the ingredients and built-up vapor pressure in the pores, particularly at temperatures around 600 °C. Following 600 °C, calcium hydroxide dehydration occurred and the aggregates began to deteriorate. As a result, the properties of the reinforced concrete were negatively affected. These effects included losses in the compressive strength and stiffness, cracking and spalling of the concrete, destruction of the bond between the cement paste and aggregates, and gradual deterioration of the hardened cement paste. The result was partial to a full loss of the structural capacity of these members and, unless strengthened, they would not be capable of carrying imposed dead and live loads.

Fig. 4 Cracking phases for NC and SCC beams under 600 °C for 1 h

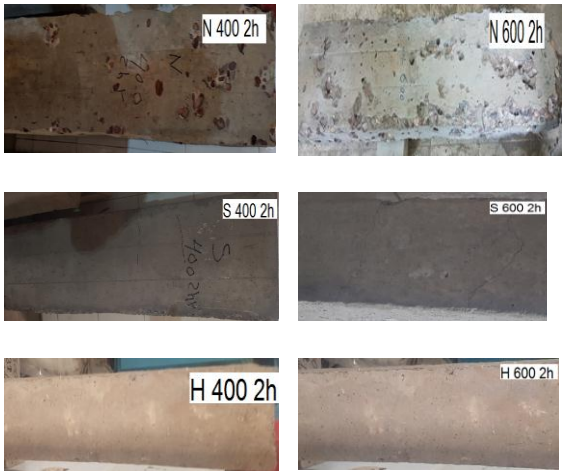

Fig. 5 Cracking phases for beams under different temperatures for 2 h exposure time

3.3. Structural Performance Of NC, SCC, And HSC Following Exposure To Different Elevated Temperature Levels

3.3.1. Crack pattern and failure mode

The NC and SCC control beams cracked after the three-point flexural test, with similar shapes and ultimate loads of the two beams. This was a result of the approximation of the NC and SCC mechanical properties. All beams failed by means of the flexural failure mode, except for the NC beams exposed to 600 °C, which exhibited shear cracks inclined at 45 degrees from the horizontal near the support. The dramatic reduction in the NC compressive strength after 600 °C changed the failure mode of these beams to shear failure. The increase in the exposure time from 1 to 2 h had a noticeable effect on the crack pattern, which appeared clearly at 600 °C. The SCC and HSC beams exhibited effective crack resistance compared to the NC beams exposed to 400 °C and 600 °C for 1 and 2 h. Increasing the exposure time to 400 °C had a noticeable effect on the failure mode of the SCC and HSC beams after testing, in contrast to the NC beams, which exhibited a significant effect, with spalling in the concrete cover, particularly after 2 h of exposure time. At the end of testing, several crushing cracks owing to compression failure appeared at the top surface. The crack width increased and the beam capacity was reduced following the elevated temperature, owing to the residual concrete strength after the elevated temperature exposure, which was substantially less than at room temperature. The average reduction in the residual concrete compressive strength was more pronounced in the NC than in the SCC and HSC. All failure modes as a result of the three-point loading system for the control beams before and after elevated

temperature exposure are illustrated in Fig. 6.

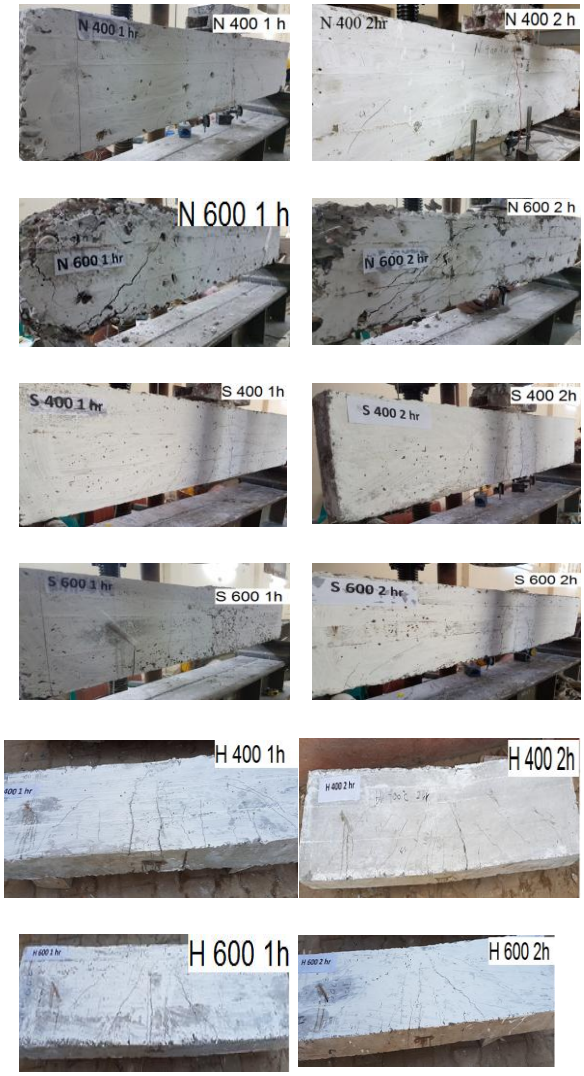

Fig. 6 Crack patterns and failure modes at different exposure times for NC, SCC, and HSC beams

3.3.2. *Effects of elevated temperature on different concrete beam types at the ultimate load capacity*

Figure 7 illustrates the ultimate failure load–temperature diagrams for un-strengthened beams exposed to elevated temperatures beams, those strengthened with CFRP, and those strengthened with steel plates. It can be observed from these curves that a reduction in the ultimate failure load occurred for the un-strengthened beams. This reduction increased as the temperature increased, but the reduction percentage was dependent on the concrete type (NC, SSC, or HSC). As the concrete became denser with lower water content (SSC and HSC), the reduction percentage decreased. The crack propagation in the SSC was limited owing to its density. The reduction in the ultimate load was very significant in the NC.

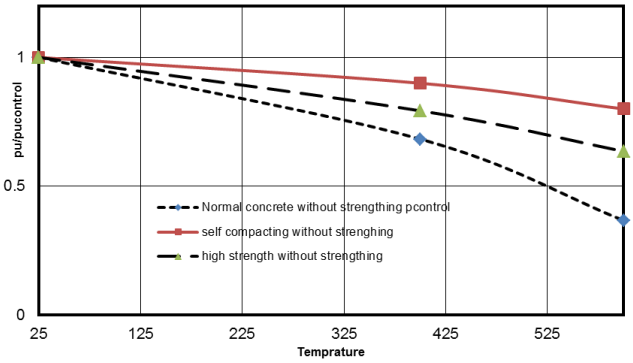

Fig. 7 Reduction in ultimate load owing to elevated temperature effect for NC, SCC, and HSC beams

3.3.3. *Elevated temperature effect on load-deflection curve*

The NC and SCC beams had approximately the same failure load, while the HSC beams underwent a 20% increase in the failure load, although the HSC compressive strength was 600 kg/cm2. The compressive strength of the HSC did not have a significant effect on the beam capacity, where the beam cross-section was the rectangular section and the failure mode was the flexural failure mode. The central deflections of the NC, SCC, and HSC beams were 4, 6, and 6.8 mm, respectively, reflecting the increase in the SCC ductility compared to the NC beams. Increasing the exposure time decreased the failure load; otherwise, the deflection curves exhibited approximately the same trend for the NC beams, as illustrated in Fig. 8. The influence of the exposure time was clear for the beam failure load, which was reduced from 82% for 1 h of exposure time to 72% following exposure to 2 h of 400 °C. This influence was represented by dramatic behavior for the NC beams under 600 °C at any exposure time, in which the beam capacity was reduced by 42% and 36% for 1 and 2 h, respectively. In the NC beams, after 400 °C, the beam capacity was reduced owing to the reduction in the concrete strength and steel reinforcement yield strength. This strength reduction can be attributed to the development of thermal stresses and the changes taking place in the physical and chemical properties of concrete. The failure load reduction of the SCC and HSC beams did not have a major effect on the beam capacity compared to the control beam after 2 h of exposure time at 400 °C. Significant reductions of the SCC beam were observed at 600 °C after 2 h of exposure time,

which reached 80% compared to the control beams, as illustrated in Fig. 9. The SCC beams exhibited strong performance compared to the NC beams. This was a result of the effective homogeneity of the SCC concrete mix and the use of dolomite as the coarse aggregate, which exhibits effective properties compared to the gravel used in the NC beams. The addition of fibres to the SCC and HSC mixes provided sufficient protection against spalling, with cracks occurring only owing to the variation in the thermal expansion of the steel and concrete. During the heating process, neither thermal nor explosive spalling was observed.

The residual compressive strength results of the tested specimens of 60 MPa following exposure to temperatures of 400 °C and 600 °C are presented in Fig. 10. The relationship between the beam capacity and exposure temperature was found to be similar to that reported previously [5]. Up to 400 °C, only a small portion of the original strength was lost, with almost the same at approximately 16% for the HSC. Severe beam capacity loss occurred mainly within the 400 °C to 600 °C range. These losses at 600 °C were in the range of 20% to 27% for 1 and 2 h, respectively. The effect of the elevated temperature on the load-deflection curve started rapidly for the HSC at 400 °C for 1 h, while the main influence of the SCC beams clearly appeared at 600 °C for 2 h.

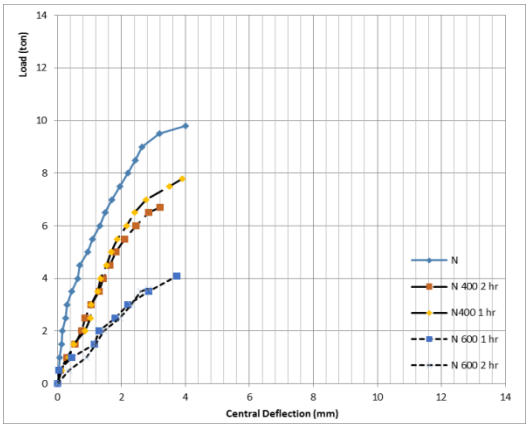

Fig. 8 Load–deflection curve for NC beams under different temperature levels and exposure times

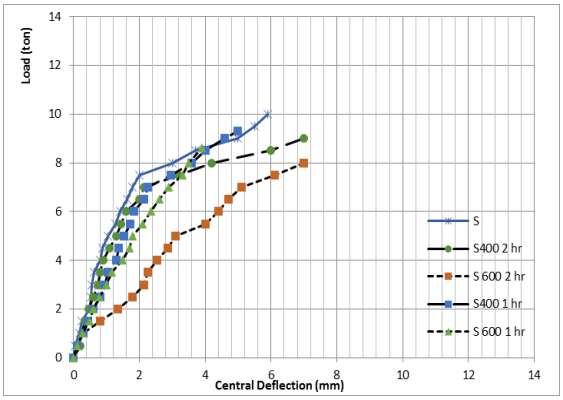

Fig. 9 Load–deflection curve for SCC beams under different temperature levels and exposure times

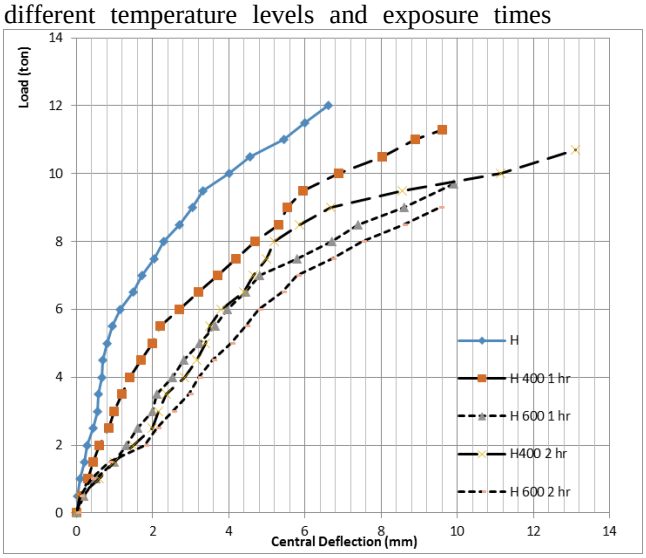

Fig. 10 Load deflection curve for high strength concrete beams under different level of temperature and different exposure time

3.3.4. *Effect of elevated temperature on the toughness of different types of concrete beams*

Figure 11 presents the toughness–temperature diagrams for exposure to a temperature of un-strengthened beams, those strengthened with CFRP, and those strengthened with steel plates. It can be observed from these curves that a reduction occurred in the toughness for the un-strengthened beams. This reduction increased as the temperature increased, but the reduction percentage was dependent on the concrete type (NC, SSC or HSC). Moreover, as the concrete became denser with lower water content (SSC and HSC), the stiffness loss became minor. The crack propagation in the SSC was limited owing to its density.

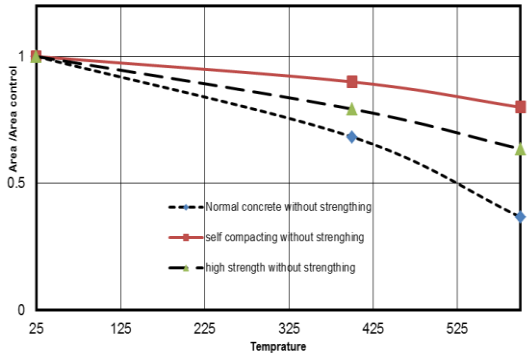

Fig. 11 Reduction in ultimate load owing to elevated temperature effect for NC, SCC, and HSC beams

4. FINITE ELEMENT MODELLING OF SPECIMENS

A solid reinforced concrete beam model, as illustrated in Fig. 12, was established using the solid 65 elements and link 8 for the steel bar simulation, as indicated in Fig. 13. All mechanical properties were considered as the experimental results before and after fire exposure. A thermal version of the model was used to calculate the temperature profile in the concrete beam; thereafter, a structural version of the model read the temperature profile to calculate the stresses. A three-dimensional (3D) eight-node tetrahedral element with a thermal degree of freedom (element type: solid 70) was selected for the heat conduction problem. The distributions of the thermal elastic stress components were then calculated by switching the solid 70 thermal elements to the solid 65 structural element, which is used for the 3D modeling of solid structures. The element is capable of plastic deformation, cracking in three orthogonal directions, and crushing. The model was created according to design considerations, with specific material properties, loadings, and boundary conditions. The study in the finite element analysis software included transient analysis and steady-state analysis (studying the structure with constant loading with varying temperatures, and varying loads with constant temperature). All numerical models were analyzed under a central load. Figures 14 to 16 present the comparisons between the theoretical and experimental results, which exhibited strong agreement for the NC, SCC, and HSC beams.

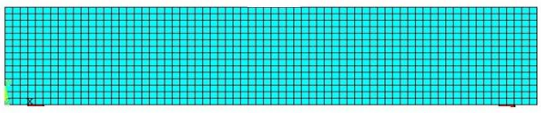

Fig. 12 3D model of tested beams

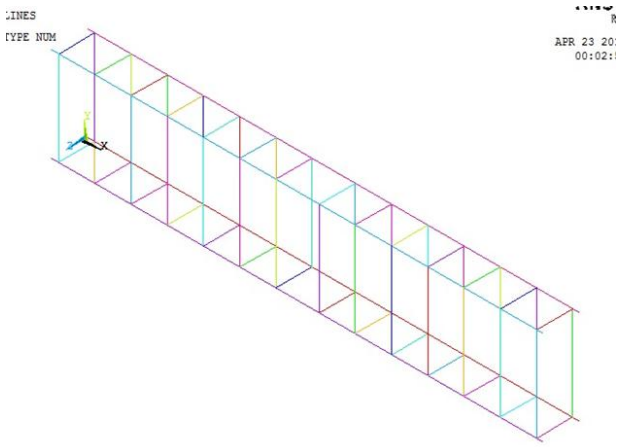

Fig. 13 Steel reinforcement modelling in finite element model

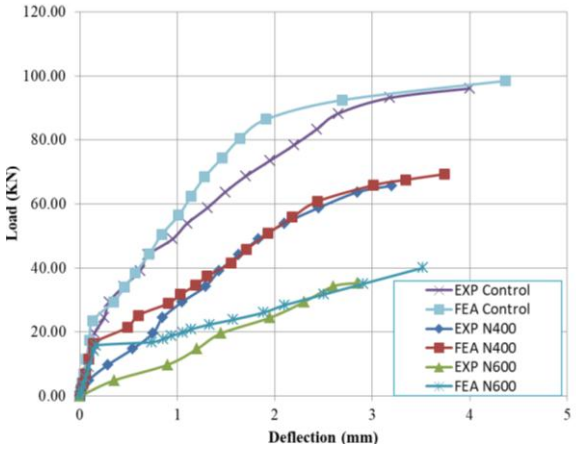

Fig. 14 Load–deflection curves of theoretical and experimental results for NC beams

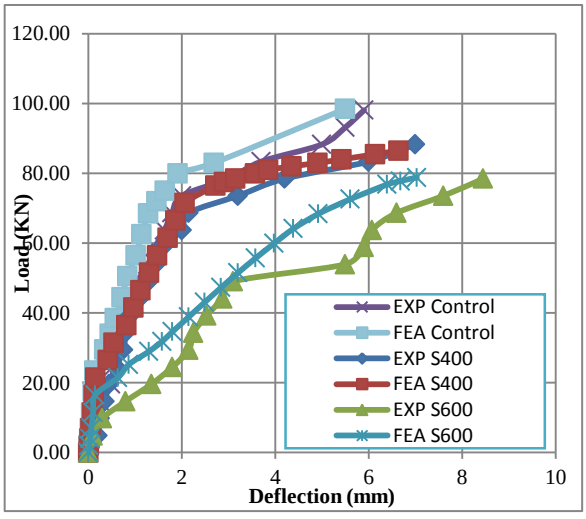

Fig. 15 Load–deflection curves of theoretical and experimental results for SCC beams

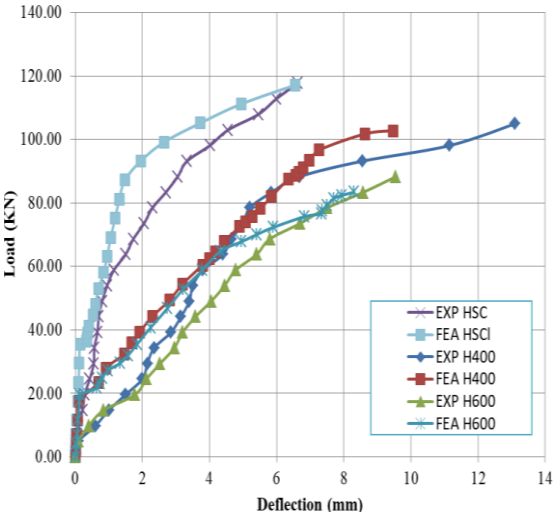

Fig. 16 Load–deflection curves of theoretical and experimental results for HSC beams

5. CONCULOSION

1- A dramatic effect was observed on the behaviour of the NC beam when increasing the exposure time of the elevated temperature, particularly with high temperature levels of more than 600 °C.
2- The SCC and HSC beams exhibited effective crack resistance compared to the NC beams when exposed to 400 °C and 600 °C for up to 2 h.
3- The crack width and numbers increased for the NC beams compared to the SCC and HSC beams after exposure to 400 °C, in addition to spalling occurring for NC only.
4- The HSC exhibited a rapid effect in the load-deflection curve after elevated temperature exposure at 400 °C for 1 h, while the SCC beams exhibited a clear effect at 600 °C for 2 h.
5- Strong agreements were observed between the experimental and theoretical results for the NC, SCC, and HSC beams.

REFERENCES

[1] Li, M., C. Qian, and W. Sun, Mechanical properties of high-strength concrete after the fire. Cement and Concrete Research, 2004. 34(6): p. 1001-1005.
[2] Noumowé, A., et al., High-Strength Self-Compacting Concrete Exposed to Fire Test. Journal of Materials in Civil Engineering, 2006. 18(6): p. 754-758.
[3] Tao, J., Y. Yuan, and L. Taerwe, Compressive Strength of Self-Compacting Concrete during High-Temperature Exposure. Journal of Materials in Civil Engineering, 2010. 22(10): p. 1005-1011.
[4] Kodur, V.K.R., B. Yu, and M.M.S. Dwaikat, A simplified approach for predicting the temperature in reinforced concrete members exposed to standard fire. Fire Safety Journal, 2013. 56: p. 39-51.
[5] Husem, M., The effects of high temperature on compressive and flexural strengths of ordinary and high-performance concrete. Fire Safety Journal, 2006. 41(2): p. 155-163.
[6] Arioz, O., Effects of elevated temperatures on properties of concrete. Fire Safety Journal, 2007. 42(8): p. 516-522.
[7] Domone, P.L., A review of the hardened mechanical properties of self-compacting concrete. Cement and Concrete Composites, 2007. 29(1): p. 1-12.
[8] Fares, H., et al., High-temperature behavior of self-consolidating concrete: Microstructure and physicochemical properties. Cement and Concrete Research, 2010. 40(3): p. 488-496.
[9] Ye, G., et al., Phase distribution and microstructural changes of self-compacting cement paste at elevated temperature. Cement and Concrete Research, 2007. 37(6): p. 978-987.
[10] Bakhtiyari, S., et al., Self-compacting concrete containing different powders at elevated temperatures – Mechanical properties and changes in the phase composition of the paste. Thermochimica Acta, 2011. 514(1): p. 74-81.
[11] Uysal, M., Self-compacting concrete incorporating filler additives: Performance at high temperatures. Construction and Building Materials, 2012. 26(1): p. 701-706.
[12] Uysal, M. and H. Tanyildizi, Estimation of compressive strength of self-compacting concrete containing polypropylene fiber and mineral additives exposed to high temperature using an artificial neural network. Construction and Building Materials, 2012. 27(1): p. 404-414.
[13] Standard, A.A.N., Standard Test Methods for Fire Tests of Building Construction and Materials. 2008.
[14] Concrete, S. and commentary (ACI 318R-11). In American Concrete Institute 2014.
[15] Abdel-Hafez, L.M., A.E.Y. Abouelezz, and A.M. Hassan, Behavior of RC columns retrofitted with CFRP exposed to fire under axial load. HBRC Journal, 2015. 11(1): p. 68-81.
[16] Elkady, H. and A. Hasan, Protection of reinforced concrete beams retrofitted by carbon fiber-reinforced polymer composites against elevated temperatures. Canadian Journal of

Civil Engineering, 2010. 37(9): p. 1171-1178.
[17] Khoury, G.A., Effect of fire on concrete and concrete structures. Progress in Structural Engineering and Materials, 2000. 2(4): p. 429-447.